scientific report

Structural and functional analysis of SGT1–HSP90 core complex required for innate immunity in plants

Yasuhiro Kadota[1], Beatrice Amigues[2], Lionel Ducassou[2], Hocine Madaoui[2], Francoise Ochsenbein[2], Raphaël Guerois[2+] & Ken Shirasu[1++]

[1]RIKEN Plant Science Center, Tsurumi-ku, Yokohama, Japan, and [2]CEA, Institut de Biologie et Technologies de Saclay (IBITECS) and CNRS, Gif-sur-Yvette, France

SGT1 (Suppressor of G2 allele of skp1), a co-chaperone of HSP90 (Heat-shock protein 90), is required for innate immunity in plants and animals. Unveiling the cross talks between SGT1 and other co-chaperones such as p23, AHA1 (Activator of HSP90 ATPase 1) or RAR1 (Required for Mla12 resistance) is an important step towards understanding the HSP90 machinery. Nuclear magnetic resonance spectroscopy and mutational analyses of HSP90 revealed the nature of its binding with the CS domain of SGT1. Although CS is structurally similar to p23, these domains were found to non-competitively bind to various regions of HSP90; yet, unexpectedly, full-length SGT1 could displace p23 from HSP90. RAR1 partly shares the same binding site with HSP90 as the CS domain, whereas AHA1 does not. This analysis allowed us to build a structural model of the HSP90–SGT1 complex and to obtain a compensatory mutant pair between both partners that is able to restore virus resistance *in vivo* through Rx (Resistance to potato virus X) immune sensor stabilization.
Keywords: molecular chaperone; co-chaperone; disease resistance; resistance protein

INTRODUCTION

Most eukaryotic organisms can recognize potential pathogens and induce defence responses to prevent disease. In higher plants, one of the most effective surveillance systems is controlled by immune sensors—the so-called resistance (R) proteins—which directly or indirectly recognize specific pathogen effectors (Jones & Dangl, 2006). The R protein homologues in animals—that is, the NOD/CATERPILLER family proteins—are also important in pathogen recognition, chronic inflammation and human diseases (Strober *et al*, 2006; Ting *et al*, 2006). Genetic and molecular biological studies have shown that, in plants, HSP90 (Heat-shock protein 90), SGT1 (Suppressor of G2 allele of skp1) and RAR1 (Required for Mla12 resistance) are the chief regulatory components of disease resistance that are triggered by many immune sensors (Schulze-Lefert, 2004). Similarly, in animals, HSP90 and SGT1 are essential for the immune responses triggered by NOD family proteins such as NOD1-dependent cytokine synthesis, NOD2-mediated activation of the transcription factor NF-κB and NALP3 (Nacht domain-, leucine rich repeat-, and PYD-containing protein 3)-mediated inflammation (Da Silva Correia *et al*, 2007; Mayor *et al*, 2007). SGT1 and HSP90 are also important for the assembly of the kinetochore complex in yeast and humans (Bansal *et al*, 2004; Steensgaard *et al*, 2004).

HSP90 (or Hsp82 in yeast)—a highly conserved eukaryotic molecular chaperone—is essential for the maturation and activation of many signalling proteins. The function of HSP90 depends on its ability to bind to and hydrolyse ATP, which is regulated by co-chaperones such as p23 and AHA1 (Activator of HSP90 ATPase 1). p23 binds to the amino-terminal domain of HSP90 (N-HSP90) and stabilizes the state required for client protein maturation or activation by slowing the rate of ATP turnover, whereas AHA1 binds to the middle domain of HSP90 and activates ATPase (Meyer *et al*, 2004; Ali *et al*, 2006).

Recently, we characterized the solution structure of the CS domain of *Arabidopsis* SGT1a that interacts with the N-HSP90. Functional analysis of the CS mutations indicated that the interaction between SGT1 and HSP90 is required for R protein accumulation and resistance against pathogens. We found that the CS domain is structurally similar to p23, suggesting that SGT1 has a similar binding property and activity as p23; however,

[1]RIKEN Plant Science Center, Suehiro-cho 1-7-22 Tsurumi-ku, Yokohama, Japan
[2]CEA, Institut de Biologie et Technologies de Saclay (IBITECS) and CNRS, Gif-sur-Yvette, France
[+]Corresponding author. Tel: +33 1 69 08 67 17; Fax: +33 1 69 08 92 75;
E-mail: raphael.guerois@cea.fr
[++]Corresponding author. Tel: +81 45 503 9574; Fax: +81 45 503 9573;
E-mail: ken.shirasu@psc.riken.jp
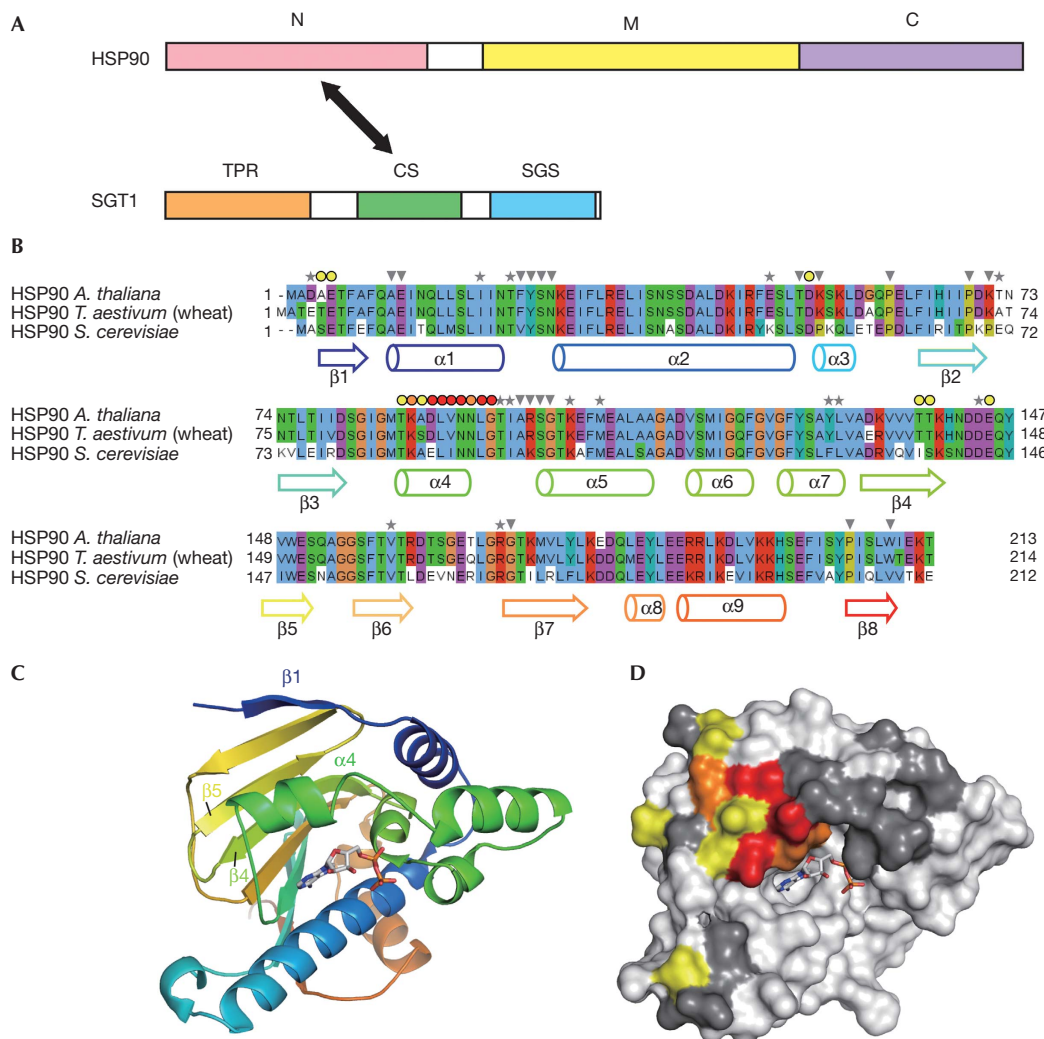
Fig 1 | Mapping of the HSP90 residues involved in the interaction with SGT1. (**A**) A schematic presentation of domain structure of SGT1 and HSP90. SGT1 consists of three domains, the TPR (a tetratricopeptide repeat) domain, the CS domain (CHORD-containing protein and SGT1) and the SGS domain (SGT1-specific motif). The CS domain binds to the amino-terminal domain of HSP90. N, M and C indicate the N-terminal, middle and carboxy-terminal domains of HSP90, respectively. (**B**) Sequence alignment of the three HSP90 proteins from *Arabidopsis thaliana* (At5g56030), *Triticum aestivum* (wheat, DQ665783) and *Saccharomyces cerevisiae* (CAA97961). Secondary structures are labelled and highlighted with respect to the domain structure shown below. The grey arrowheads indicate the residues the resonances of which were not observed in the NMR spectra. The grey asterisks indicate the residues assigned in the free form but not unambiguously identified in the bound form. The filled circles indicate the residues the ^{15}N and ^{1}H chemical shifts of which were perturbed by the addition of the CS domain from yellow ($0.2 > \Delta\delta$p.p.m. > 0.14) and orange ($0.26 > \Delta\delta$p.p.m. > 0.2) to red ($\Delta\delta$p.p.m. > 0.26). (**C**) Schematic representation of the N-terminal domain of yeast Hsp90 (N-Hsp90) structure with an ADP molecule represented as sticks (Protein Data Bank: 1AMW). (**D**) Surface representation of the N-Hsp90 domain in the same orientation as in panel **C** with the surface coloured from yellow to red with respect to the intensity of the chemical shifts on addition of the CS domain (see above legend for filled circles in panel **B**). The dark grey residues indicate the positions that were not unambiguously identified (corresponding to the grey asterisks and arrowheads in panel **B**). HSP90, Heat-shock protein 90; NMR, nuclear magnetic resonance; SGT1, Suppressor of G2 allele of skp2.

the CS domain does not affect the ATPase activity of HSP90 (Botër *et al*, 2007).

Understanding the structure of the SGT1–HSP90 complex is crucial to explain the molecular mechanism of how it functions with immune sensors. Here, we generated a three-dimensional model structure of the complex by using the HADDOCK program

and data from nuclear magnetic resonance (NMR)-based interaction surface mapping and mutational analyses. Surprisingly, although structurally similar to p23, SGT1 binds to a surface of HSP90 different from the surface corresponding to the p23-binding site. Both the TPR and SGS domains of SGT1 indirectly compete with p23 for binding to HSP90, thereby explaining the

difference between the effects of SGT1 and p23 on the ATPase activity of HSP90, and suggesting that SGT1 acts as a unique co-chaperone of HSP90.

RESULTS AND DISCUSSION
SGT1 binds to a new co-chaperone-binding site of HSP90

To study the structure and function of the SGT1–HSP90 complex, the region of HSP90 that interacts with the CS domain of SGT1 was mapped by NMR using the previously assigned N-terminal domain of *Saccharomyces cerevisiae* Hsp82 (N-ScHsp82; Salek *et al*, 2002) and the CS domains of *S. cerevisiae* Sgt1 (ScSgt1) or *Arabidopsis* SGT1a (AtSGT1a) produced in *Escherichia coli*. We reassigned 95% of the backbone N, C and H atoms of yeast Hsp82 (supplementary Fig S1A online). The ^{1}H-^{15}N heteronuclear single quantum coherence (HSQC) experiment provides a fingerprint of the protein structure the cross-peaks of which are sensitive to any structural or environmental variation on binding of a partner. The unlabelled yeast CS domain was added progressively to an N-ScHsp82 ^{13}C/^{15}N-labelled sample up to a molar ratio of 1:3 between N-ScHsp82 and CS-ScSgt1. Perturbations in the N-ScHsp82 resonances were monitored from the ^{1}H-^{15}N HSQC and triple-resonance three-dimensional experiment recordings. The ^{15}N and ^{1}H resonances of a restricted set of amino acids were notably affected (supplementary Fig S1B online). Mapping their positions on the surface of N-ScHsp82 resulted in a continuous surface patch, which probably accounts for the interaction surface between the two domains (Fig 1). The core—the most perturbed region of this interface—corresponded to the α4 helix. The surrounding positions in the strand β1, the acidic loop between the strands β4 and β5, and the short α3 helix were affected but to a lesser extent. By using the titration signals of L89, L93 and G94 as probes, we extracted a mean K_d value of $27 \pm 3\,\mu$M (supplementary Fig S2). We also monitored the formation of a heterologous complex between the N-ScHsp82 domain and the CS domain of AtSGT1a (CSa), and found that the same residues in N-ScHsp82 were the most perturbed, with some differences in the weakly affected residues (E4 and T85; supplementary Fig S3A,B). In the presence of 150 mM NaCl, the same resonances were found to be perturbed on CS titration (supplementary Fig S3C,D).
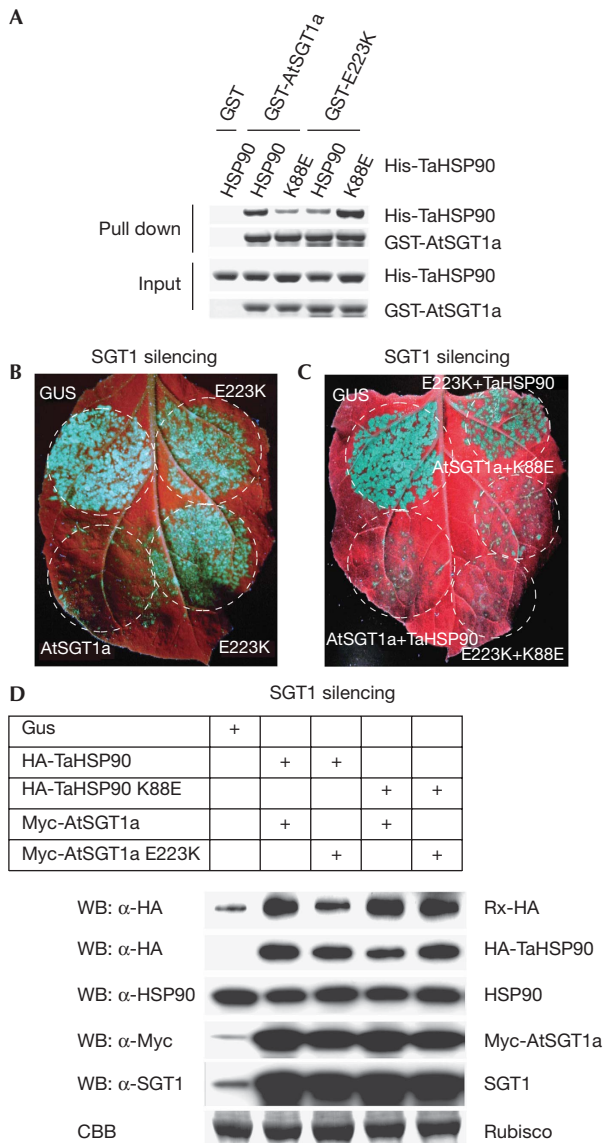
The amino acids involved in the interaction were defined further by site-directed mutagenesis of HSP90 using wheat (*Triticum aestivum*) HSP90 (TaHSP90), which has 91% amino acid similarity to yeast Hsp82 and is highly soluble *in vitro*. We achieved eight single amino-acid substitutions in TaHSP90 for solvent-exposed residues that are located inside the surface affected by SGT1 binding. On the basis of the glutathione S-transferase (GST) pull-down experiments, the mutations E6R, T87E, K88E, D90R, N93R, D145R and E146R disrupted the ability of TaHSP90 to bind to CSa, full-length AtSGT1a or AtSGT1b *in vitro*, whereas the R100E mutation enhanced the ability (Fig 2A; supplementary Fig S1A,B online). To check the conservation of this interaction across species, we made equivalent mutations in the N-terminal domain of yeast Hsp82. K86E (K88E in TaHSP90) and D143R (D145R in TaHSP90) reduced the binding to CSa, as well as CS of ScSgt1 (supplementary Fig S5 online).

The region defined by these mutations is a new co-chaperone interaction site of HSP90, as other well-known co-chaperones
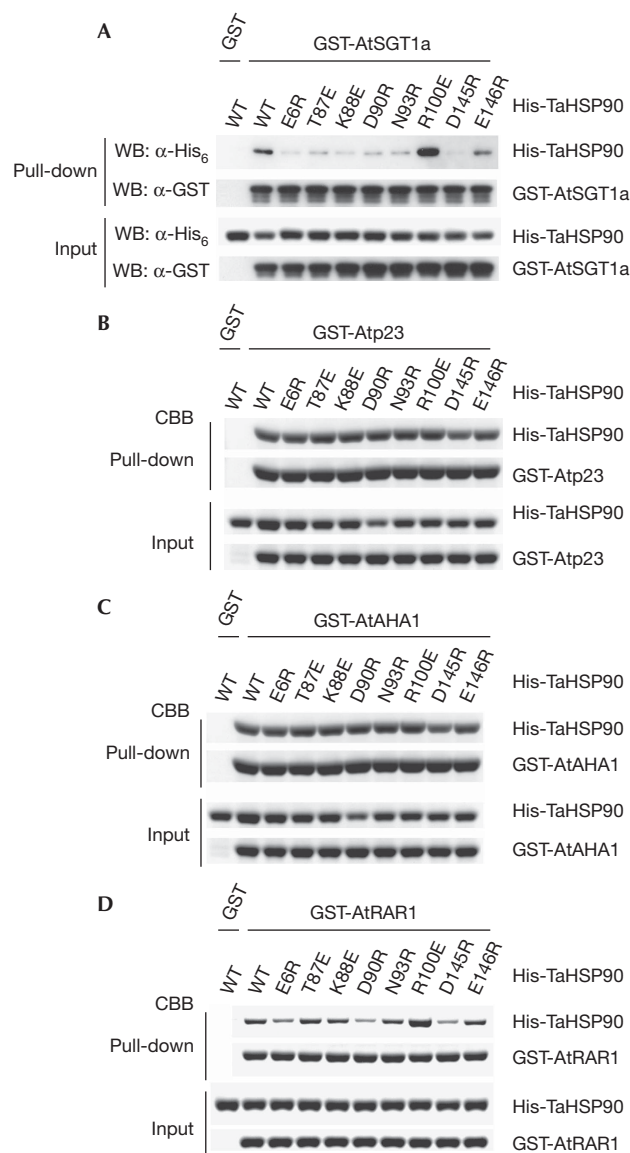
Fig 2 | *In vitro* interaction assays between co-chaperone and HSP90 mutants. The glutathione S-transferase (GST) fusion co-chaperones (**A**) AtSGT1a, (**B**) Atp23, (**C**) AtAHA1 and (**D**) AtRAR1 were incubated with purified His 6-TaHSP90 or mutants as indicated. The pulled-down fractions were analysed by using SDS–polyacrylamide gel electrophoresis followed by the Coomassie blue staining or immunoblotting using α-His 6 and α-GST antibodies as indicated. For the pull-down assay with GST-Atp23, 2 mM AMP-PNP was added to both the pull-down and washing buffers to enhance HSP90 binding. AHA1, Activator of HSP90 ATPase 1; At, *Arabidopsis thaliana*; CBB, Coomasie brilliant blue; HSP90, Heat-shock protein 90; RAR1, Required for Mla12 resistance; SGT1, Suppressor of G2 allele of skp2; Ta, *Triticum aestivum*; WB, Western blot; WT, wild type.

such as p23 (yeast Sba1) and AHA1 bind to different regions (see below). Consistently, none of the mutations affected the binding of HSP90 to *Arabidopsis* orthologues p23 (Atp23) and AHA1 (AtAHA1) *in vitro* (Fig 2B,C). However, E6R, D90R and D145R reduced the binding of HSP90 to *Arabidopsis* RAR1 (AtRAR1),

Fig 3 | The K88E mutation in *Triticum aestivum* HSP90 complements the loss of function of the E223K mutant of *Arabidopsis thaliana* SGT1a. (**A**) *In vitro* interaction assays between the K88E mutant of TaHSP90 and the E223K mutant of AtSGT1a. GST-AtSGT1a or GST-E223K were incubated with purified His 6-TaHSP90 or the His 6-K88E mutant of TaHSP90 as indicated, and the pulled-down fractions were analysed by using SDS–polyacrylamide gel electrophoresis followed by the Coomassie blue staining. (**B**) Functional assay of E223K in Rx-mediated resistance against potato virus X (PVX). Rx-HA-expressing *Nicotiana benthamiana* silenced for *NbSGT1* were co-infiltrated with *Agrobacterium* expressing *Myc-E223K* and *PVX-GFP* (optical density (OD), 0.3 and 0.001). *Myc-AtSGT1a* (positive) and *GUS* (negative) were used as controls. PVX accumulation was monitored by green fluorescent protein (GFP) fluorescence under ultraviolet illumination at 5 days after inoculation. The residue numbers correspond to the *T. aestivum* HSP90 sequence. (**C**) The K88E mutation in HSP90 complemented the loss of function of the E223K of AtSGT1a in Rx-mediated resistance against PVX. *Myc-AtSGT1a* or *Myc-E223K* and *HA-TaHSP90* or *HA-K88E* were coexpressed with *PVX-GFP* by *Agrobacterium* (OD 0.3, 0.3 and 0.001) in Rx-HA-expressing *N. benthamiana* plants silenced for *NbSGT1*. Note that transient expressions of Myc-AtSGT1a restored the resistance regardless of the presence of HA-TaHSP90 or HA-K88E, probably because the Myc-AtSGT1a protein can function with endogenous HSP90. (**D**) The K88E mutation in HSP90 compliments the reduced accumulation of Rx caused by the E223K mutation in AtSGT1a. The expression of the proteins were checked by immunoblotting using α-HA, α-HSP90, α-Myc and α-SGT1 antibodies. At, *Arabidopsis thaliana*; CBB, Coomasie brilliant blue; GST, glutathione *S*-transferase; HA, haemagglutinin; HSP90, Heat-shock protein 90; SGT1, Suppressor of G2 allele of skp2; Ta, *Triticum aestivum*; WB, Western blot.

another protein required for immune sensor function (Fig 2D), suggesting that in contrast to p23 and AHA1, the HSP90 region where SGT1 binds partly overlaps the RAR1-binding surface. Consistently, binding to the CHORD-I domain of RAR1 was also reduced in these mutants (supplementary Fig S4C online), confirming the earlier report that the CHORD-I domain competes with SGT1 for HSP90 binding (Botër *et al*, 2007).

A pair of HSP90 and SGT1 mutations restores resistance

The SGT1–HSP90 binding interface was confirmed by searching for mutants that showed specific charge compensation effects. We tested six CSa mutants—R153D, E155K, K159D, K170D, K221E and E223K—for which binding to TaHSP90 was notably weaker, with five TaHSP90 mutants—E6R, K88E, D90R, D145R and E146R (supplementary Fig S6 online). Only one of these mutations, namely E223K in AtSGT1a and K88E in TaHSP90, restored the binding between both partners, from either the isolated CSa domain or the full-length AtSGT1a (Fig 3A;

supplementary Fig S6 online). This suggests that K88 in TaHSP90 binds to E223 in TaHSP90 or at least that these amino acids are located close to each other on the interface. Consistently, the K86E mutation in the N-terminal domain of yeast Hsp82, which is equivalent to K88E in AtSGT1a, also complemented the reduced binding of E223K mutant in CSa (supplementary Fig S7 online).

To test whether these mutants also showed a compensatory effect *in planta*, we depleted the endogenous SGT1 amounts by virus-induced gene silencing in *Nicotiana benthamiana* plants containing a haemagglutinin (HA)-tagged immune sensor, Rx, to confer resistance against the potato virus X (PVX; Azevedo *et al*, 2006). In this line, we transiently expressed Myc-tagged AtSGT1a, Myc-E223K or β-glucuronidase (GUS) with green fluorescent protein (GFP)-tagged PVX. The Myc-AtSGT1a protein restored the resistance, preventing PVX-GFP accumulation (Fig 3B). By contrast, the Myc-E223K protein did not complement the loss of endogenous SGT1, allowing PVX-GFP accumulation to levels similar to those of the GUS control (thus susceptible). Next, we coexpressed Myc-AtSGT1a or Myc-E223K with HA-TaHSP90 or HA-K88E and analysed the resistance against PVX-GFP (Fig 3C). The Myc-E223K/HA-K88E combination restored the resistance against PVX-GFP, whereas the Myc-E223K/HA-TaHSP90 combination did not. We obtained the same results with Myc-E231K in AtSGT1b, another copy of SGT1 in *Arabidopsis* (supplementary Fig S8 online). Rx resistance was restored by the Myc-E223K/HA-K88E pair probably owing to the recovery of the Rx protein levels as shown in the protein blot analysis (Fig 3D). In conclusion, the direct interaction of SGT1 with the new co-chaperone-binding
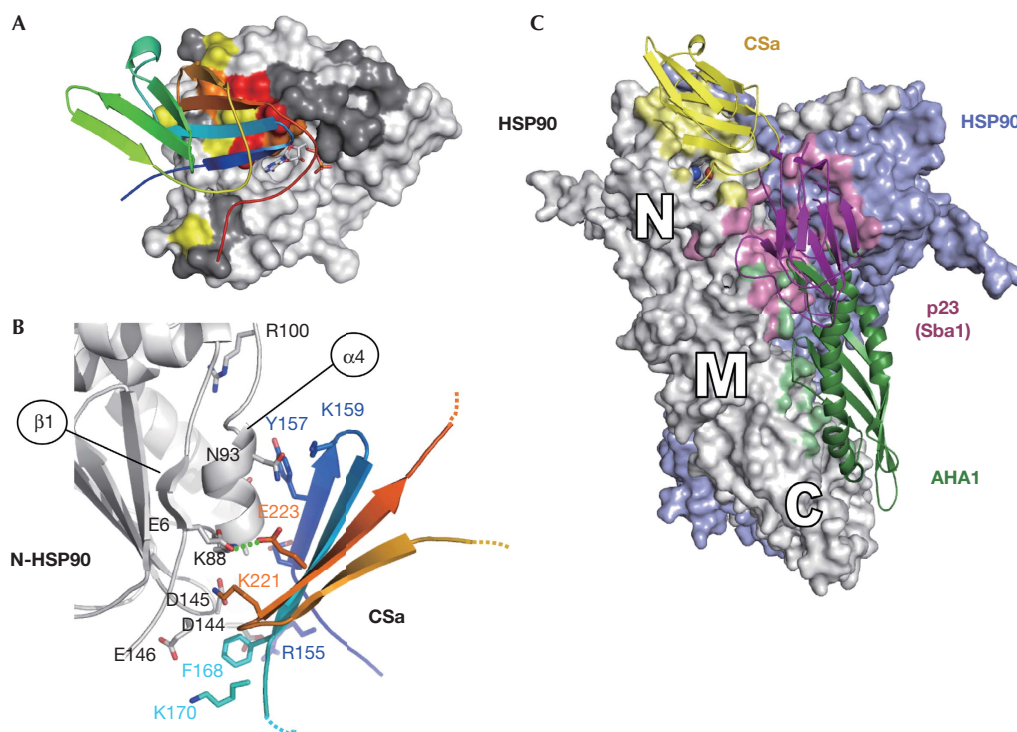
Fig 4 | Structural model of the SGT1–HSP90 complex. (**A**) Representation of the lowest energy model of cluster 1 obtained from docking under nuclear magnetic resonance constraints between the CSa domain (rainbow coloured) and the amino-HSP90 (surface coloured with the chemical shift perturbation index; see Fig 1B). (**B**) Detailed view of the interface of the modelled complex. Side chains mutated or discussed in the text are shown as sticks and labelled in black for HSP90 and in colour for CSa. The residue numbers correspond to the *Triticum aestivum* HSP90 sequence. (**C**) The model built from the assembly of the HSP90 dimer (each monomer in grey and light blue shown on the surface) in complex with yeast p23 (Sba1; purple ribbon), AHA1 bound to the middle domain of HSP90 (green ribbon) and the CS-SGT1 domain docked to the N-terminal domain of HSP90 (yellow ribbon). The surface of contact of each HSP90 monomer with these co-chaperones is coloured with the same colour code as their ribbons. N, M and C indicate the N-terminal, middle and carboxy-terminal domains of HSP90, respectively (drawn with PyMOL; http://pymol.sourceforge.net). AHA1, Activator of HSP90 ATPase 1; HSP90, Heat-shock protein 90; SGT1, Suppressor of G2 allele of skp2.

site in HSP90 is crucial for stabilizing the immune sensor Rx and its resistance to PVX.

Structural model of the CS–HSP90 complex

By using the HADDOCK docking program (see Methods), we performed a docking simulation to explore further the possible structural arrangements that are compatible with the interface residues identified from the NMR and mutational analyses. Initially, no specific restraints were applied to the CS–E223/HSP90–K88 compensatory pair to check for the robustness of the docking simulation; only two solutions were found to entirely satisfy the spatial constraints (supplementary Fig S9 online). Of the two, only one cluster accounted for the charge compensation effect between K88E in TaHSP90 and E223K in AtSGT1a (Fig 4A,B). In the lowest energy model, the side chains of E223 and K88 point towards the same side of the helix, and the tips of their side chains are only 2.6 Å apart (Nζ-Oε2 distance). E223, located just at the periphery of the interface, might readily compensate for a charge reversal in K88; therefore, the E223–K88 compensation effect supports the model that represents a mode of association between CS and N-HSP90.

Further inspection of the lowest energy structure shows that the interface of 1,390 Å² comprises a central hydrophobic patch between $Y157_{SGT1a}$, $V164_{SGT1a}$ and $A87_{HSP90}$ that is surrounded by a group of charged interactions located near the N terminus of the CS domain. A consistent set of charge complementarities can be observed at the interface for the mutated charged residues in AtSGT1a ($R153_{SGT1a}$-$D144_{HSP90}$, $E155_{SGT1a}$-$K57_{HSP90}$, $K170_{SGT1a}$-$E146_{HSP90}$, $K221_{SGT1a}$-$D145_{HSP90}$ and $E223_{SGT1a}$-$K88_{HSP90}$). Most of these side chains are found to be highly conserved throughout evolution, emphasizing the consistency of these networks.

Steric hindrance in co-chaperone-binding modes to HSP90

We constructed a global model with yeast p23 and AHA1 superimposed onto the CSa–HSP90 complex (using Protein Data Bank codes 2CG9 and 2USV; Fig 4C). The binding interface between HSP90 and p23 (shown in purple) overlaps largely with that of AHA1 (shown in green), resulting in structural and functional competition between the two co-chaperones for HSP90 binding (Harst *et al*, 2005). CSa has a two-layered β-sandwich structure similar to that of p23, and the HSP90-binding sites of CSa and p23 are on the same side (Fig 4C; Botër *et al*, 2007). However, our results showed that both SGT1 and p23 bind to distinct sites of the HSP90. The contact surfaces of CSa and p23 in HSP90 seem to be contiguous but not overlapping. Consistent with the model, the CSa domain did not compete with p23 for HSP90 binding (Fig 5A), and
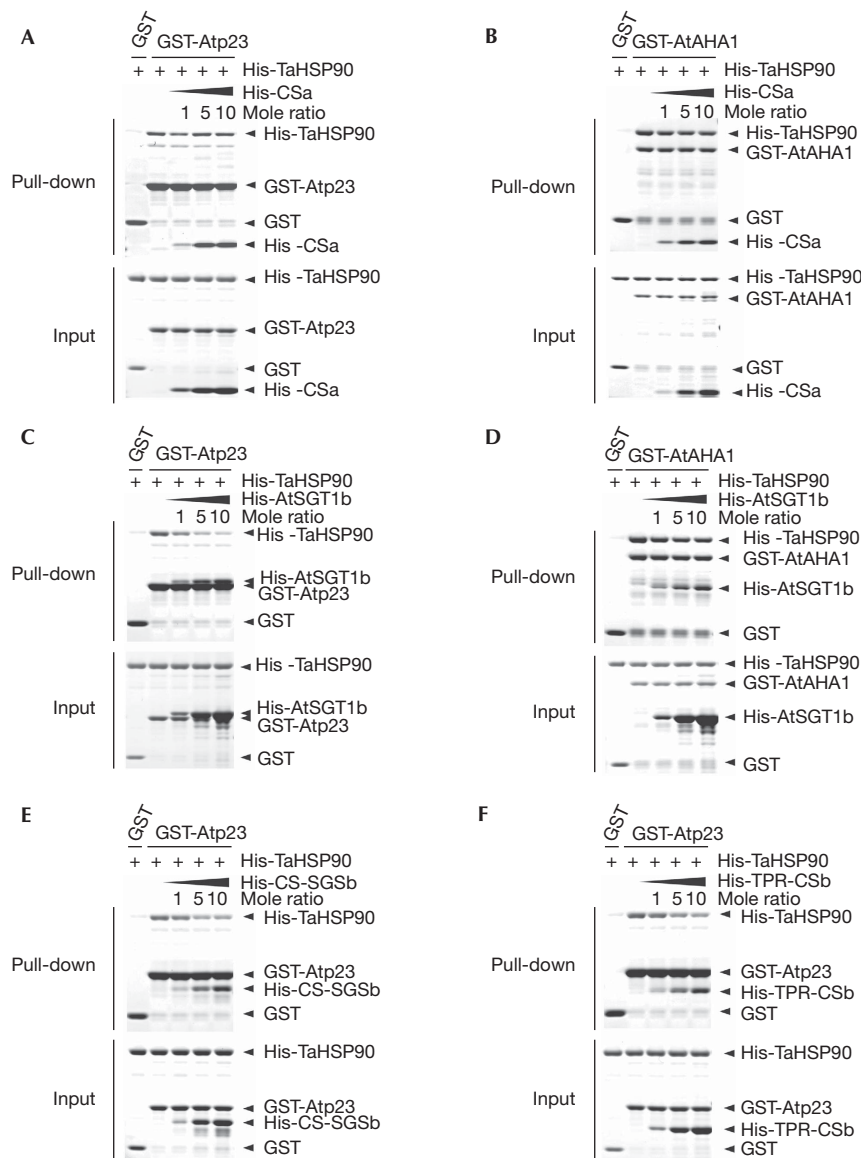
Fig 5 | Competition assay of the CSa domain and *Arabidopsis thaliana* SGT1b with Atp23 and AtAHA1. (A,B) The CSa domain did not compete with p23 and AtAHA1 for binding to *Triticum aestivum* HSP90. GST-Atp23 or GST-AHA1 were incubated with His 6-TaHSP90 in the absence or presence of increasing amounts of purified His 6-CSa as indicated. For the pull-down assay with GST-Atp23, 2 mM AMP-PNP was added to both the pull-down and washing buffers. The GST-pulled down fractions were analysed by using SDS–polyacrylamide gel electrophoresis and the Coomassie blue staining. **(C,D)** Full-length AtSGT1b competed with p23 but not with AtAHA1 for binding to TaHSP90. **(E,F)** Both TPR and SGS domains, but not the CS domain competed with Atp23 for TaHSP90 binding. AHA1, Activator of HSP90 ATPase 1; GST, glutathione *S*-transferase; HSP90, Heat-shock protein 90; SGT1, Suppressor of G2 allele of skp2.

remote from each other, neither did AHA1 and CSa (Fig 5B). Next, we assessed whether full-length SGT1 competes with Atp23 and AtAHA1 for HSP90 binding using AtSGT1b rather than AtSGT1a because of the higher affinity of the former for TaHSP90 *in vitro*. Although neither CSa nor CSb inhibited the binding of Atp23 to TaHSP90, AtSGT1b inhibited this binding in a concentration-dependent manner (Fig 5C; supplementary Fig S10 online). The unexpected inhibition is caused by the N-terminal TPR and the carboxy-terminal SGS domains of SGT1, as TPR-CSb and CS-SGSb fragments perturb the Atp23–TaHSP90 interaction (Fig 5E,F), indicating that although the binding sites of HSP90 with SGT1

and p23 are different, these two proteins are unlikely to function simultaneously. By contrast, the AtAHA1 interaction with TaHSP90 was not perturbed by AtSGT1b (Fig 5D). As a control, we showed that neither AtSGT1b nor AtRAR1 could bind to AtAHA1 or Atp23 (supplementary Fig S11 online).

SGT1 and p23 bind to distinct regions of HSP90 but still compete with each other for binding, suggesting that SGT1 functions differently from p23. When ATP binds to the N-terminal domain, the HSP90 homodimer forms a closed conformation by association of the N-terminal domains. p23 preferentially binds to HSP90 in the presence of ATP or the non-hydrolysable ATP

analogue AMP-PNP and stabilizes the closed conformation by inhibiting ATPase activity (Siligardi *et al*, 2004). By contrast, CSa does not affect the ATPase activity of HSP90 (Botër *et al*, 2007). Furthermore, the binding of SGT1 to HSP90 is unaffected by AMP-PNP but is enhanced by geldanamycin (supplementary Fig S12 online), whereas geldanamycin inhibits p23 binding to HSP90 (Sullivan *et al*, 1997). The different binding site of HSP90 and the distinct nature of SGT1 as compared with p23 suggest a new mode of action of this co-chaperone, which is consistent with the recently discovered function of SGT1 that would bridge both the HSP70 and HSP90 systems through various domains (Spiechowicz *et al*, 2007; Nöel *et al*, 2007). Further investigations should enlighten the detailed mechanisms by which the TPR and SGS domains contribute to the function of HSP90.

METHODS

NMR spectroscopy. NMR experiments of uniformly labelled N-ScHsp82 (1–210) were performed on Bruker Advance 2 600- and 700-MHz spectrometers at 298 K and those for resonance assignment, using 1 mM protein (pH 8) and 10 mM Tris. Sequential backbone resonance assignments were achieved by using standard 15N-1H-HSQC, HNCA, CBCA(CO)NH, HBHA(CO)NH, NOESY (nuclear Overhauser enhancement spectroscopy)-HSQC, and TOSCY (total correlated spectroscopy)-HSQC experiments. NMR titration was performed using 15N-labelled N-ScHsp82 domain (1–210) (1.7 mM; Tris 20 mM, pH 8) and the unlabelled CS domain of either *S. cerevisiae* Sgt1 (176–290) or AtSGT1a (149–253) (0.8 mM) at 293 K.

Pull-down assays. We incubated 10 µg of the GST fusion proteins with the same molar ratio of His 6-tagged proteins in the pull-down buffer (20 mM HEPES-KOH, pH 7.5; 50 mM KCl; 5 mM MgCl$_2$; 1% Tween20; 50 µM ZnCl$_2$, 40 mM NaCl; 1 mM DTT; and 100 µM phenylmethylsulphonyl fluoride) at 4 °C for 1 h. The GST fusion proteins were pulled down using 50% glutathione sepharose 4 FF (GE Healthcare UK Ltd, Buckinghamshire, UK), washed four times with the pull-down buffer and eluted with 10 mM glutathione. The bound, His 6-tagged proteins were analysed by using SDS–polyacrylamide gel electrophoresis and the Coomassie blue staining or immunoblotting as indicated.

Docking simulation. HADDOCK v1.3 (Dominguez *et al*, 2003) was applied using default settings to dock together the structural models generated as described online in the Supplementary methods.

Supplementary information is available at *EMBO reports* online (http://www.emboreports.org).

REFERENCES
Ali MM, Roe SM, Vaughan CK, Meyer P, Panaretou B, Piper PW, Prodromou C, Pearl LH (2006) Crystal structure of an Hsp90-nucleotide-p23/Sba1 closed chaperone complex. *Nature* **440:** 1013–1017

Azevedo C, Betsuyaku S, Peart J, Takahashi A, Nöel L, Sadanandom A, Casais C, Parker J, Shirasu K (2006) Role of SGT1 in resistance protein accumulation in plant immunity. *EMBO J* **25:** 2007–2016

Bansal PK, Abdulle R, Kitagawa K (2004) Sgt1 associates with Hsp90: an initial step of assembly of the core kinetochore complex. *Mol Cell Biol* **24:** 8069–8079

Botër M *et al* (2007) Structural and functional analysis of SGT1 reveals that its interaction with HSP90 is required for the accumulation of Rx, an R protein involved in plant immunity. *Plant Cell* **19:** 3791–3804

Da Silva Correia J, Miranda Y, Leonard N, Ulevitch R (2007) SGT1 is essential for Nod1 activation. *Proc Natl Acad Sci USA* **104:** 6764–6769

Dominguez C, Boelens R, Bonvin AM (2003) HADDOCK: a protein–protein docking approach based on biochemical or biophysical information. *J Am Chem Soc* **125:** 1731–1737

Harst A, Lin H, Obermann WM (2005) Aha1 competes with Hop, p50 and p23 for binding to the molecular chaperone Hsp90 and contributes to kinase and hormone receptor activation. *Biochem J* **387:** 789–796

Jones JD, Dangl JL (2006) The plant immune system. *Nature* **444:** 323–329

Mayor A, Martinon F, De Smedt T, Petrilli V, Tschopp J (2007) A crucial function of SGT1 and HSP90 in inflammasome activity links mammalian and plant innate immune responses. *Nat Immunol* **8:** 497–503

Meyer P, Prodromou C, Liao C, Hu B, Roe SM, Vaughan CK, Vlasic I, Panaretou B, Piper PW, Pearl LH (2004) Structural basis for recruitment of the ATPase activator Aha1 to the Hsp90 chaperone machinery. *EMBO J* **23:** 1402–1410

Nöel LD, Cagna G, Stuttmann J, Wirthmuller L, Betsuyaku S, Witte CP, Bhat R, Pochon N, Colby T, Parker JE (2007) Interaction between SGT1 and cytosolic/nuclear HSC70 chaperones regulates *Arabidopsis* immune responses. *Plant Cell* **19:** 4061–4076

Salek RM, Williams MA, Prodromou C, Pearl LH, Ladbury JE (2002) Backbone resonance assignments of the 25 kD N-terminal ATPase domain from the Hsp90 chaperone. *J Biomol NMR* **23:** 327–328

Schulze-Lefert P (2004) Plant immunity: the origami of receptor activation. *Curr Biol* **14:** R22–R24

Siligardi G, Hu B, Panaretou B, Piper PW, Pearl LH, Prodromou C (2004) Co-chaperone regulation of conformational switching in the Hsp90 ATPase cycle. *J Biol Chem* **279:** 51989–51998

Spiechowicz M, Zylicz A, Bieganowski P, Kuznicki J, Filipek A (2007) Hsp70 is a new target of Sgt1—an interaction modulated by S100A6. *Biochem Biophys Res Commun* **357:** 1148–1153

Steensgaard P, Garre M, Muradore I, Transidico P, Nigg EA, Kitagawa K, Earnshaw WC, Faretta M, Musacchio A (2004) Sgt1 is required for human kinetochore assembly. *EMBO Rep* **5:** 626–631

Strober W, Murray PJ, Kitani A, Watanabe T (2006) Signalling pathways and molecular interactions of NOD1 and NOD2. *Nat Rev Immunol* **6:** 9–20

Sullivan W, Stensgard B, Caucutt G, Bartha B, McMahon N, Alnemri ES, Litwack G, Toft D (1997) Nucleotides and two functional states of hsp90. *J Biol Chem* **272:** 8007–8012

Ting JP, Kastner DL, Hoffman HM (2006) CATERPILLERs, pyrin and hereditary immunological disorders. *Nat Rev Immunol* **6:** 183–195